Of course the missile acceleration and guidance error histories will be different in the two cases, if only because the metric law gives an indefinite number of histories from the time to go at which the controller is activated.

In the relatively general case[9,10] where $\phi_{nn}(s)=k_n^2$ (white metric noise) and $\phi_{TT}(s)=k_{T_p}^2/s^{2p}$, the Wiener-Hopf equation giving $W(s)$ and $X_0(s)$ has an analytical solution. The poles of $W(s)$, $X_0(s)$, and $M_0(s)$ follow a Butterworth configuration of degree $p+2$ with $\omega=(k_{T_p}/k_n)^{1/(p+2)}$. $M_0(s)$ is given by

$$M_0(s)=\frac{m_1 s^{p+1}+2m_2 s^{p+2}+\ldots+(p+1)m_{p+1}s+(p+2)\omega^{p+2}}{s^{p+2}+m_1 s^{p+1}+\ldots+m_{p+1}s+\omega^{p+2}} \tag{13}$$

where m_i are the coefficients of the Butterworth polynomial. The miss distance is $\sigma_d^2=m_1 k_n^2$. In the angular case, the proportional navigation ratio is $p+2$.

Clearly, in most cases, the optimal angular guidance filter $C_0(s)=M_0(s)S^{-1}(s)P^{-1}(s)$ is not realizable. In contrast, the optimal metric law is always realizable.

Conclusion

Linear-Quadratic-Gaussian optimization, without constraint on commanded acceleration and with stationary measurement and process noise, yields the same theoretical minimum miss distance irrespective of whether the control law is angular or metric. Generally, however, the optimal angular law cannot be realized exactly. If an approximate angular law such as simple proportional navigation is used, the resulting performance degradation is inversely proportional to measurement noise. The metric law produces a performance advantage as a result of time-to-go measurement, which produces a better missile lateral acceleration history against a maneuvering target. As is known, the specific problems of radome design and seeker-to-missile coupling[1] are such that the implementation of an optimal control law is more effective in the case of command-to-line-of-sight guidance than with homing guidance.[10]

References

[1]Nesline, F.W. and Zarchan, P., "A New Look at Classical Versus Modern Homing Missile Guidance," *Proceedings of the Conference on Guidance and Control,* AIAA, New York, AIAA, New York, 1979, pp. 230-242.

[2]Lanning, J. and Battin, R., *Random Processes in Automatic Control,* Mc-Graw Hill Book Co., New York, 1956.

[3]Zarchan, P., "Complete Statistical Analysis of Nonlinear Missile Guidance Systems SLAM," *Journal of Guidance, Control, and Dynamics,* Vol. 2, Jan. 1979, pp. 71-78.

[4]Bennet, R.R. and Mathews, W.E., "Analytical Determination of Miss Distances for Linear Homing Navigation Systems," Hughes Aircraft Co., Tech. Memo. 260, March 1952.

[5]Nesline, F.W. and Zarchan, P., "Miss Distance Dynamics in Homing Missiles," *Proceedings of the Conference on Guidance and Control,* AIAA, New York, 194, pp. 84-98.

[6]Bryson, A. E. Jr. and Ho., Y.C., *Applied Optimal Control,* Hemisphere Publishing Corp., 1975, pp. 158-167, pp. 422-428.

[7]Price, C.F., "Application of Optimal Control Techniques to Tactical Missile Guidance," AGARD AG 251, 1981, pp. 13.1-13.18.

[8]Stallard, D.V., "Discrete Optimal Control Solutions, with Application to Missile Guidance," *Proceedings of the Conference on Guidance and Control,* AIAA, New York, 1984, p. 335-346.

[9]Vergez, P.L. and Liefer, R.K., "Target Acceleration Modeling for Tactical Missile Guidance," *Journal of Guidance, Control and Dynamics,* Vol. 7, May-June 1984, pp. 315-321.

[10]Durieux, J.L., "Terminal Control for Command to Line of Sight Guided Missile," AGARD LS 135, pp. 4.1-4.14.

On-Off Attitude Control of Flexible Satellites

S. B. Skaar,* L. Tang,† and I. Yalda-Mooshabad†
Iowa State University, Ames, Iowa

Introduction

THE reorientation of a satellite is often more rapidly achieved using thrusters rather than internal momentum transfer devices. However, thrusters have the disadvantages of being difficult to adjust with precision and of tending to excite elastic modes of vibration. Feedback control schemes[1] have been offered for thruster control based on pulse-width and pulse-frequency modulation. If, however, control moment gyros or other internal mechanisms are available to take over the fine control once the maneuver is complete, an open-loop approach for thruster-based attitude acquisition may be useful. Open-loop control will be especially attractive if the switching times can be selected in such a way as to effectively minimize the postmaneuver elastic energy of the system.

The present work is an examination of the relationship between post maneuver elastic energy and switch time selection. It is conducted in the context of a simple satellite model that has served as the basis for other flexible space structure control studies.[2,3] The control is restricted in that only three switching times can be selected: 1) time T_1, the duration of the first thrust interval; 2) time T_2 at which a braking interval begins; and 3) time T_3 at which the braking interval ends. A final time T_F, measured from the beginning of the first thrust interval, is specified before which the maneuver is to be completed.

Assuming that the system begins from rest, two requirements are placed upon the maneuver: 1) a prescribed angular impulse (resulting in the desired final system angular velocity) should be delivered, and 2) a prescribed time integral of the angular impulse is to be delivered at T_F. In the absence of an additional constraint or condition, an infinite number of switch time combinations T_1, T_2, and T_3 could be selected such that the maneuver is completed by time T_F. The selection of this third condition is shown to have a significant impact upon the final presence or absence of elastic energy.

The Model

Consider the rigid hub and flexible appendage model of Fig. 1. If the four cantilevered appendages are elastic, of constant cross section, and relatively long and thin, then the equations that govern the response of the angular position $\theta(t)$ of the rigid hub and that of the appendage deflection $y(z,t)$ to the control torque u are given by

$$I_T\left(\frac{\mathrm{d}^2\theta}{\mathrm{d}t^2}\right)+4\rho\int_{R_i}^{R_o} z\left(\frac{\partial^2 y}{\partial t^2}\right)\mathrm{d}z=u \tag{1}$$

$$EI\left(\frac{\partial^4 y}{\partial z^4}\right)+\rho\left[\left(\frac{\partial^2 y}{\partial t^2}\right)+z\left(\frac{\mathrm{d}^2\theta}{\mathrm{d}t^2}\right)\right]=0 \tag{2}$$

Received Aug. 8, 1985; revision received Jan. 13, 1986.

*Assistant Professor, Department of Engineering Science and Mechanics. Member AIAA.

†Graduate Student, Department of Engineering Science and Mechanics.

with

$$y(R_i,t)=\frac{\partial y}{\partial z}(R_i,t)=\frac{\partial^2 y}{\partial z^2}(R_o,t)=\frac{\partial^3 y}{\partial z^3}(R_o,t)=0 \quad (3)$$

where I_T is the total rigid-body mass moment of inertia of the system about its axis of rotation and the physical parameters ρ, EI, R_i, and R_o are defined as indicated in Fig. 1.

The "average" angular position of the system θ_A is defined in terms of the angular position of the hub θ and the appendage defelctions $y(z,t)$ according to

$$\theta_A=\theta+\left(\frac{4\rho}{I_T}\right)\int_{R_i}^{R_o} zy\,dz \quad (4)$$

In the absence of deflections, θ and θ_A are the same. It follows from Eqs. (1) and (4) that

$$I_T\ddot{\theta}_A=u \quad (5)$$

Equation (5) provides two of the criteria for selecting the three switching times T_1, T_2, and T_3 illustrated in Fig. 2. If values of θ_A and $\dot{\theta}_A$ are prescribed at $t=T_F$, according to

$$\theta_A(T_F)=\theta_{AF} \quad (6)$$

$$\dot{\theta}_A(T_F)=\dot{\theta}_{AF} \quad (7)$$

then it can be shown from Eq. (5) that the switching times T_1, T_2, and T_3 must satisfy

$$T_3=T_1+T_2-\dot{\theta}_{AF}I_T/u_M \quad (8)$$

$$T_2=\frac{\theta_{AF}-\dot{\theta}_{AF}^2 I_T/2u_M-\dot{\theta}_{AF}T_F}{T_1u_M/I_T-\dot{\theta}_{AF}} \quad (9)$$

Thus, the selection of T_1 determines T_2 and T_3 from Eqs. (9) and (8), respectively. The time T_1 is not unrestricted, however, and must fall within bounds given by

$$T_{1_{\min}}\le T_1\le T_{1_{\max}} \quad (10)$$

where the selection of $T_1=T_{1_{\min}}$ coincides with the minimum-fuel choice ($T_3=T_F$) and the selection of $T_1=T_{1_{\max}}$ coincides with the minimum-time choice ($T_1=T_2$).

The Selection of T_1

A reasonable criterion for the selection of T_1 subject to the restrictions of Eqs. (8-10) would be the degree of elastic energy remaining in the system following the maneuver. Let $\dot{g}(t)$ be the response of the angular velocity of the hub $\dot{\theta}(t)$ to a unit impulse. If the system begins from an undeformed state of rest, then the subsequent, angular velocity history is related to the input control torque $u(t)$ according to

$$\dot{\theta}(t)=\int_0^t u(\lambda)\dot{g}(t-\lambda)\,d\lambda \quad (11)$$

Furthermore, the increment of work dW done on the system by the torque u over an increment of time dt is given by

$$dW=u\dot{\theta}\,dt=u\int_0^t u(\lambda)\dot{g}(t-\lambda)\,d\lambda\,dt \quad (12)$$

If $u(t)$ is of the form shown in Fig. 2, then the total work done on the system by the control torque over the time interval, $0\le t\le T_F$, is

$$W=\int_0^{T_F} u\dot{\theta}\,dt=u_M^2\left[\int_0^{T_1}\int_0^t \dot{g}(t-\lambda)\,d\lambda\,dt-\int_{T_2}^{T_3}\left(\int_0^{T_1}\dot{g}(t-\lambda)\,d\lambda-\int_{T_2}^{t}\dot{g}(t-\lambda)\,d\lambda\right)dt\right] \quad (13)$$

In the absence of dissipation mechanisms, such as viscoelastic material damping, the work W of Eq. (13) is equal to the sum of the kinetic and elastic energies remaining in the system at T_F. This final energy can be broken down into two parts,

$$W=\tfrac{1}{2}I_T\dot{\theta}_{AF}^2+E_R \quad (14)$$

where the first term on the right is the rigid-body kinetic energy and E_R is that part of the postmaneuver energy due to elastic vibration.

Of interest here is the dependence of E_R upon the choice of T_1 [subject to Eqs. (8) and (9)]. To ascertain this relationship for the model of Fig. 1, the impulse response $\dot{g}(t)$ used in Eq. (13) must be found. A method similar to that detailed in Ref. 4 for a simpler, but analogous, system is used.

First, the Laplace transformation of Eqs. (1-3) is taken resulting in

$$I_T s^2\Theta+4\rho s^2\int_{R_i}^{R_o} zY(z)\,dz=U \quad (15)$$

$$EI(d^4Y/dz^4)+\rho s^2 Y=-\rho z s^2\Theta \quad (16)$$

with

$$Y(R_i)=\frac{dY}{dz}(R_i)=\frac{d^2Y}{dz^2}(R_o)=\frac{d^3Y}{dz^3}(R_o)=0 \quad (17)$$

where the upper-case variable names Θ, $Y(z)$, and U are the Laplace transformations of the lower case $\theta(t)$, $y(z,t)$, and $u(t)$. The general solution to the fourth-order ordinary differential equation (16) can be written

$$Y(z)=\Theta[e^{\beta z}(A\cos\beta z+B\sin\beta z)+e^{-\beta z}(C\cos\beta z+D\sin\beta z)-z] \quad (18)$$

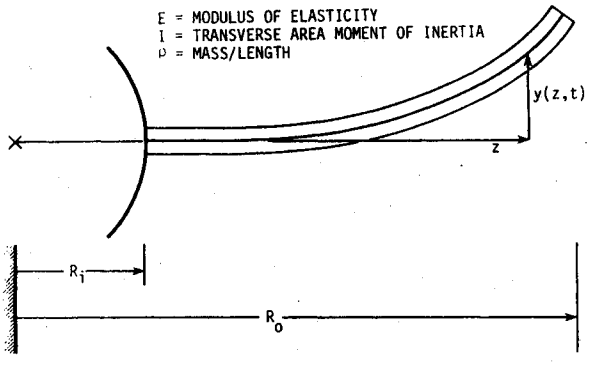

Fig. 1 Satellite model.

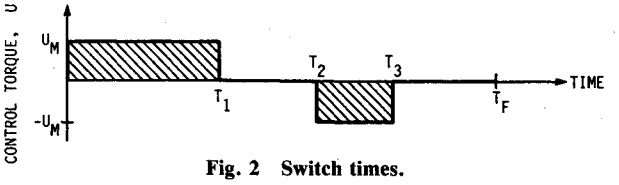

Fig. 2 Switch times.

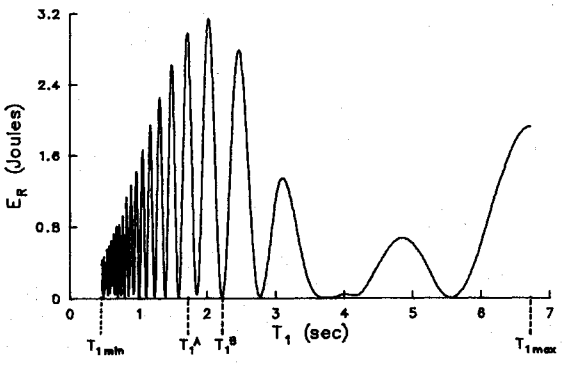

Fig. 3 Elastic energy vs T_1, rest-to-rest maneuver.

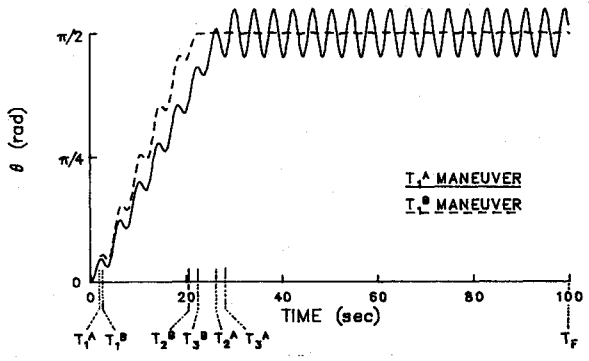

Fig. 4 Hub angle response.

where the somewhat involved evaluation of the constants A, B, C, and D is made using the transformed boundary conditions of Eq. (17). Equation (18) is then substituted into the integral of Eq. (15) and that integral is solved analytically. With this integral solved, the transformed base angle Θ appears linearly in each term on the left side of Eq. (15), allowing for evaluation of the transfer function as follows:

$$\frac{s\Theta}{U} = \mathcal{L}\{\dot{g}(t)\} = \frac{\beta^3}{s}\{e^{2\beta R_i} + e^{2\beta R_o}[4(s_i s_o + c_i c_o)^2 + 2]$$

$$+ e^{2\beta(2R_o - R_i)}\}\{I_0\beta^3[e^{2\beta R_i} + e^{2\beta R_o}(4(s_i s_o + c_i c_o)^2 + 2)$$

$$+ e^{2\beta(2R_o - R_i)}] + 2\rho[e^{2\beta R_i}(-2\beta^2 R_i^2 + 2\beta R_i - 1)$$

$$+ e^{2\beta R_o}[(8\beta^2 R_i^2 - 4)((s_o^2 - c_o^2)s_i c_i - (s_i^2 - c_i^2)s_o c_o)$$

$$+ 4\beta R_i(c_i s_o - s_i c_o)^2 - (c_i c_o + s_i s_o)^2]$$

$$+ e^{2\beta(2R_o - R_i)}(2\beta^2 R_i^2 + 2\beta R_i + 1)]\}^{-1} \quad (19)$$

where I_0 is the mass moment of inertia of the rigid hub about the axis of rotation and

$$\beta = (\rho s^2/4EI)^{1/4} \quad (20)$$

$$s_i = \sin\beta R_i \quad (21)$$

$$s_o = \sin\beta R_o \quad (22)$$

$$c_i = \cos\beta R_i \quad (23)$$

$$c_o = \cos\beta R_o \quad (24)$$

The impulse response of interest $\dot{g}(t)$ is found by evaluating the inverse Laplace transformation of Eq. (19) using the method of residues.[5] Thus,

$$\dot{g}(t) = \frac{1}{I_T} + \sum_{j=1}^{\infty} C_j \exp(s_j t) + \bar{C}_j \exp(\bar{s}_j t) \quad (25)$$

and $s_j = i\omega_j$ (along with its complex conjugate $\bar{s}_j = -i\omega_j$) are the imaginary poles of Eq. (19). The complex coefficients C_j are found from Eq. (19) according to

$$C_j = \lim_{s \to s_j} \frac{(s - s_j)s\Theta}{U} \quad (26)$$

The series of Eq. (25) must be truncated at some point before the input energy determined from Eq. (13) can be evaluated. Equation (13) seems to converge adequately with the inclusion of a small number of terms.

Table 1 Physical parameters used in the test case

I_0 = 66.27 N·m·s^2	ω_1 = 1.55 rad/s
I_T = 287.31 N·m·s^2	ω_2 = 5.32 rad/s
R_i = 0.50 m	ω_3 = 14.21 rad/s
R_o = 8.50 m	ω_4 = 27.65 rad/s
ρ = 0.27 kg/m	ω_5 = 45.64 rad/s
EI = 57.46 N·m^2	ω_6 = 68.11 rad/s

A Rest-to-Rest Example

The physical parameters used for the example are given in Table 1. The torque level u_M is 10 N·m and the final time T_F is 100 s. The angle θ_{AF} is required to reach a value of $\pi/2$ by $t = T_F$, with $\dot{\theta}_{AF} = 0$.

Six terms from the series of Eq. (25) were retained to assess the relationship of the postmaneuver vibrational energy (E_R) with the first switch time T_1, subject to Eqs. (6-10). The first six natural frequencies corresponding to the poles of Eq. (19) are reported in Table 1. A plot indicating the relationship between T_1 and E_R is shown in Fig. 3. Clearly, the choice of T_1 is significant. Several values or value ranges of T_1 appear to be good selections from the standpoint of low elastic energy. The centers of the broadest intervals of T_1, which result in relatively low energy levels, appear to be particularly attractive selections from the point of view of minimizing the adverse effect of actuation error.

Three types of impulse response variations were investigated to determine the sensitivity of the lowest energy T_1 values to modeling error: 1) sensitivity to the number of modes included, 2) error in the frequencies, and 3) error in the values of the complex coefficients C_i and $\bar{C}_i$ of Eq. (25). In all three cases, a plot similar to that of Fig. 3 was constructed, with only the particular variation of interest in the impulse response model to account for disparities with Fig. 3. Error in the frequencies appeared to be of some significance, but neither errors on the order of 5% in the coefficients nor the use of two rather than six modeled modes were sufficient to result in switch time selections that would produce significantly altered residual elastic energy.

To visualize the impact of the T_1 selection upon the motion of the flexible body, two different plots of angular position θ of the hub versus time are superimposed in Fig. 4. The first is the result of the selection of time T_1^A and the second is the result of the selection of time T_1^B (both located in Fig. 3). The angular position calculation is based upon a convolution integral like that of Eq. (11), where

$$\theta(t) = \int_0^t u(\lambda)g(t-\lambda)\,d\lambda \quad (27)$$

Six natural frequencies are retained in the impulse response function g for the purpose of generating Fig. 4.

Conclusions and Remarks

Impulse response functions are shown to be a potentially useful tool for the selection of control switch times in the bang-bang attitude control of linear, elastic, slewing satellites. Experimentally acquired impulse responses may be suitable for this purpose, since indicated switch times (which result in relatively low postmaneuver vibrational energy) do not appear to be overly sensitive to identification error (with the exception of frequency error). The adverse effects of actuation error upon postmaneuver elastic energy levels can be reduced if longer control bursts associated with switch times closer to the minimum-time rigid-body solution are favored over shorter bursts near the minimum-fuel solution. This is due to the fact that the low-energy troughs are significantly broader close to the minimum-time solution. The magnitude of the energy peaks, however, is lower for T_1 values selected near the minimum-fuel solution.

Acknowledgment

This work was supported by the National Science Foundation under Grant MEA-8318867.

References

[1]Wie, B. and Barba, P. M., "Quaternion Feedback for Spacecraft Large Angle Maneuvers," AIAA Paper 84-1032, May 1984.

[2]Breakwell, J. A., "Optimal Feedback Slewing of Flexible Spacecraft," *Journal of Guidance and Control*, Vol. 4, Sept.-Oct. 1981, pp. 472-479.

[3]Turner, J. D. and Chun, H. M., "Optimal Distributed Control of a Flexible Spacecraft During a Large-Angle Maneuver," *Jounal of Guidance, Control, and Dynamics*, Vol. 7, May-June 1984, pp. 257-264.

[4]Skaar, S. B., "Closed Form Optimal Control Solutions for Continuous Linear Elastic Systems," *Journal of the Astronautical Sciences*, Vol. 32, No. 4, Oct.-Dec., 1984.

[5]Wylie, C. R., *Advanced Engineering Mathematics*, McGraw-Hill Book Co., New York, 1975.